

CONDUCTION PROCESSES IN THICK FILM RESISTORS PART I

M. P. ANSELL

Glass Division, Standard Telecommunication Laboratories Limited, London Road, Harlow, Essex, England

(Received April 29, 1976)

The structures of three families of thick film resistors have been investigated by scanning electron microscopy and electron probe micro-analysis. The two principal components of the resistive glazes, that is the conducting pigment and the glassy binder, have been identified in each case. The pigments were found to be simple or ternary oxides of the Pt transition metal group and Pd/PdO/Ag alloys. The glassy binders were based on lead borosilicate glasses.

A model for the electronic conduction processes through the glass and pigments is proposed on the basis of the observed physical structures, the measured electrical properties of resistors and the properties of the component resistor materials.

Part I of the total paper is concerned with identifying the phases in various Thick Film Resistors and part II considers the conduction processes that are appropriate.

1 INTRODUCTION

The properties of a good thick film resistor (TFR) system should be reproducible in manufacture and stable over a wide range of temperatures and applied fields. The conditions of firing, preferably in air, and precision control of ink composition should not be of crucial importance in a good system. In practice typical specifications for a system are a resistance range between 10 Ω /square and 1 M Ω /square, a temperature coefficient of resistance (TCR) of less than ± 100 ppm/K, a noise level of less than ± 30 dB/decade and an environmental stability of less than 1% drift per 1000 hours at 150°C. Resistor systems are known to be based on combinations of a conducting pigment and a glass where the desired resistivity is obtained by varying the proportion of one component to the other with the possible inclusion of additives. It is surprising that TCRs are so low in TFR materials when the definitions of TCR are considered.

For a *metal*, where the TCR is high and positive, the resistance R is given by

$$R = R_0(1 + \alpha T),$$

where α is the TCR and it is always ≥ 100 ppm/K, R_0 is a constant and T is temperature.

A negative TCR implies *semiconducting* behaviour when

$$R = R_0 \exp\left(\frac{E}{kT}\right),$$

where E is the activation energy for conduction and k is Boltzmann's constant. Differentiating,

$$\frac{dR}{dT} = -R_0 \exp\left(\frac{E}{kT}\right) \left(\frac{E}{kT^2}\right) = -\frac{RE}{kT^2}$$

By definition,

$$\text{TCR} = \frac{1}{R} \frac{dR}{dT} = -\frac{E}{kT^2} \text{K}^{-1}.$$

At 300K a negative TCR of < 100 ppm K^{-1} is equivalent to $E < 800 \mu\text{eV}$. Thus a material which conducts with this value of TCR requires $E < 1$ meV, that is $kT/25$ at room temperature. Such a material cannot be considered as a simple semiconductor. Possible multi-phase materials with the required range of electrical properties are now discussed.

Experimental measurements made by Cash¹ in fact show the members of three TFR systems to have activation energies of $< kT$ over the temperature range from 10K to 300K. Within an acceptable range of working temperatures about room temperature, TCRs are in the range ± 100 ppm/K with $E < kT/20$. A simple metal or semiconductor cannot therefore be used as the conducting phase.

The required conductivity of TFR material is calculated for a resistor 1 cm square by 30 μm thick. For a resistance of 10 Ω the material conductivity is $3.3 \times 10^1 \Omega^{-1} \text{cm}^{-1}$ and for a 1 M Ω resistor the conductivity is $3.3 \times 10^{-4} \Omega^{-1} \text{cm}^{-1}$. At room temperature materials having this range of conduc-

tivities are semiconductors except for the high conductance material which lies just in the range of metals and semi-metals. Conduction in semiconductors takes place via a small and highly temperature dependent density of carriers with high mobility. In a metal electrons are free to move in an energy range of the order of 4 kT about the Fermi level. Electrons travelling through a metallic crystal under the influence of an applied field are impeded by scattering processes arising from lattice vibrations, impurities, defects and other carriers. All metals have positive TCRs in excess of 1000 ppm K⁻¹ and are thus unsuitable not only on account of the magnitude of the resistivity but also on account of its temperature dependence.

An alternative material source for low TCR resistors could be a disordered solid containing many carriers but with low mobility. Effectively the material has a narrow localised conduction band where conditions for conduction are relatively temperature independent. Conduction takes place via energetically close sites with limitations imposed by the physical distance between the sites. Hypothetical phase structures which could exist within a TFR to give low TCR values are listed below:

(1) A disordered material containing trapping sites created by doping and by the inherent disorder. Here the conductivity is controlled by the doping level.

(2) An insulating material containing metallically conducting particles, rather than ions, closely spaced or touching (0 to 50 Å) which were either

- (i) initially present in the prefired mix and remained unchanged during the firing cycle, or

(ii) crystallised out from solution during the cooling part of this cycle.

(3) A very low TCR metal-like phase in an insulating phase where some continuous conduction paths, through the metal-like material only, exist and the conductivity of the resistor is determined by the number of these paths.

(4) Combinations of (1), (2) and (3).

Two courses of experimental action are therefore required to determine the conduction processes which occur in commercial TFR systems. It is necessary to observe any phase structure and to identify the materials in each case, and also to measure the electrical properties of these resistors. By these methods it should be possible to determine how the TCRs of resistor systems are kept low over a wide range of resistivities.

2 EXPERIMENTAL

Resistors, fired according to the manufacturer's specifications, were kindly supplied by Dr. P. Holmes of RAE Farnborough. The resistor inks were all commercial compositions fired on to approximately 96% pure alumina substrates in two standard test patterns. The fired resistor inks investigated are listed in Table I together with their code designations and ohms per square ratings.

Observation of resistor surfaces by eye showed high resistivity components to have a glazed finish whereas low resistivity material had a matt appearance. The surface of matt resistors can generally be damaged by a sharp instrument, whereas high resistivity material is resistant to scratching.

Resistors were embedded face upwards in araldite and the glazed surface layer was lapped away to a depth of about 5 μm to reveal any possible microstructure. The resistor surfaces were then successively polished with abrasive pastes from 6 μm to 0.25 μm particle size, using the standard techniques employed in the preparation of geological specimens. After removal from the araldite, samples were etched for 15 seconds in a solution of one volume of HF to five volumes of de-ionized water, in order to remove surface contamination. This improved the surface definition for microscopy without destroying any structural detail.

A Jeol JXA 50A scanning electron microscope (SEM) with an electron-probe micro-analyser (EPMA) facility linked to an X-ray energy dispersive elemental analysis system, were used to evaluate the resistor surfaces. Transversely fractured resistors were also

TABLE I
Resistors investigated

Series	Resistor code	Ohms/square	
Du Pont	1111	10	
	1100	1121	100
		1131	1 k
		1141	10 k
		1151	100 k
		1161	1
Alloys B	R11B	10	
	R12B	100	
	R13B	1 k	
	R14B	10 k	
	R15B	100 k	
Electroscience	7013	1 k	
	7000	7014	10 k

viewed in section to ensure that their structure was uniform through the resistor bulk. Polished resistor material was resolvable up to a magnification of about $\times 10,000$ with a depth of field of about $7\ \mu\text{m}$. At $\times 1000$ the depth of field is about $100\ \mu\text{m}$. Specimens were observed uncoated except for very high conductivity material which received a $400\ \text{\AA}$ (approx.) coating of carbon to eliminate charging.

Characteristic X-rays excited from the specimen's component elements are distinguished according to their energies rather than their wavelengths. The resolution of the detector, however, is limited to $200\ \text{eV}$ by electronic noise. The energy spectra are displayed on a multi-channel analyser and spectral data may be stored and manipulated by a mini-computer. Energy dispersive analysis is less accurate than wavelength dispersive analysis but has the advantages of high speed and flexibility.

The electron probing beam diameter is up to $1\ \mu\text{m}$ in size but because the transmission power of X-rays into materials is generally larger than that of electrons, the size of an X-ray emission area is far larger than the diameter of the electron probe, that is between 1 and $3\ \mu\text{m}$. Hence when probing areas of less than $3\ \mu\text{m}$ in diameter with a stationary electron beam a background due to surrounding material can be expected. A further problem is caused by peaks, of say a K excitation, overlapping with another peak of an L or M excitation which complicates simple elemental analysis. Nevertheless energy dispersive analysis was sufficiently selective for the purpose of this work.

3 RESULTS

Micrographs showing the phase structure of the three resistor systems under investigation are now described. The result of elemental analysis on the observed phases follow the micrographs for each resistor series.

3.1 *Du Pont 1100 Series*

3.1.1. Micrographs Figure 1 shows a section through a 1111 resistor surface in which there is a large void. Angular-shaped particles, assumed to be crystallites are discernible in the void area (Figure 2) and range in size from sub-micron to $3\ \mu\text{m}$. Bright areas on the resistor surface are charged dust particles. Figure 3 shows the polished, unetched sample surface. Crystalline particles, in contact, are embedded in a

darker matrix material which is identified as a glass phase from spectra described later.

Figure 4 for the $100\ \Omega/\text{square}$ resistor shows a similar pattern to Figure 1 except that the composite material is now more continuous with fewer voids (Figure 5). There is slightly lower density of crystallites, and $0.1\ \mu\text{m}$ particles are resolvable (Figure 6).

Only small voids are apparent in Figure 7 for the Du Pont 1131 composition. Etching has brought out the surface particles in greater relief (Figure 8) as now there is more glassy material to be etched away. A section of a transversely fractured, unpolished 1131 resistor (Figure 9) shows a $15\ \mu\text{m}$ thick TFR layer bonded to an alumina substrate. The white crystallites, up to $4\ \mu\text{m}$ in width, are seen to be very nearly touching, consistent with the more two-dimensional polished surface of Figure 8. The large void on the right of Figure 9 has a crystallite-free region below it which has the appearance of a bubble rising up through the resistor. This might occur during the firing process, with the bubble displacing crystallites and leaving liquid glass and small debris to flow in behind it until cooling of the resistor locked the bubble in as a void.

Figures 10, 11, 12, 13, 14, and 15 show a further decrease in the crystallite density as the resistivity increases from $10\ \text{k}\Omega$ to $1\ \text{M}\Omega$ for 1141, 1151, and 1161 resistors.

3.1.2. Spectra Spectra for all Du Pont 1100 resistors show the particulate material to have an excess of Bi and Ru over the matrix phase which contains more Pb and Si. Spectra for the two phases in Du Pont 1161 are shown in Figure 16. Note the position of the Pb and Bi L peaks in each spectrum and the Ru K peak in the crystalline material. In accordance with chemical analysis carried out on these resistor inks by Coleman and Graves² the crystalline phase can be tentatively classed as bismuth ruthenate and the intermediate phase as a lead borosilicate glass.

An exception to the two phase structure is 1131 where some crystallites give a clear Ag L α peak, and because of a small background count they can be identified as pure silver. Figures 5 and 8 show a rather sudden transition in particle spacings in 1121 and 1131. The expected increase in resistivity caused by the decrease in particle density is probably lessened by the addition of highly conducting silver particles. This addition may also stabilise or adjust the TCR value for 1131. Dupont 1141 contains no silver but a small Cd peak is detected from the glassy phase

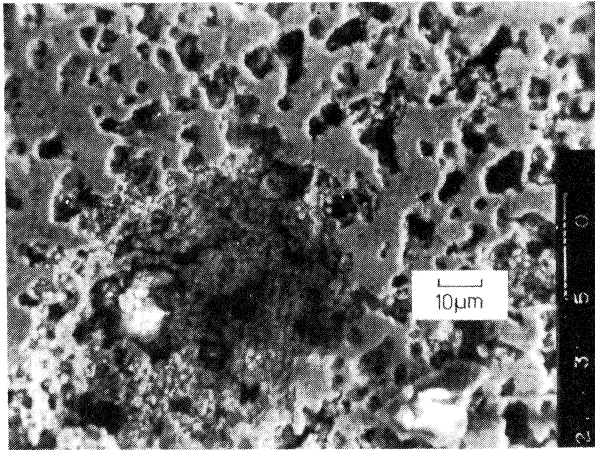


FIGURE 1 Du Pont 1111

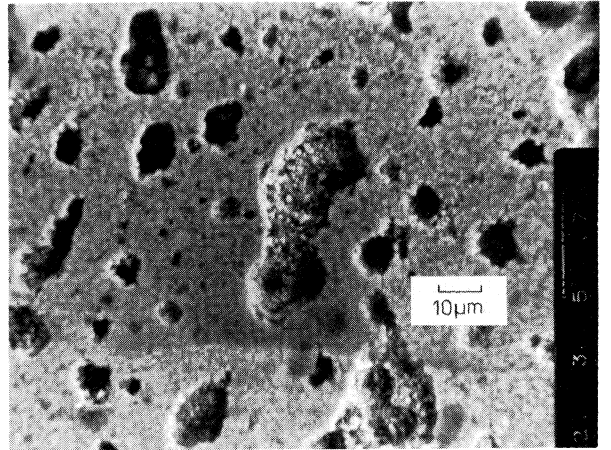


FIGURE 4 Du Pont 1121

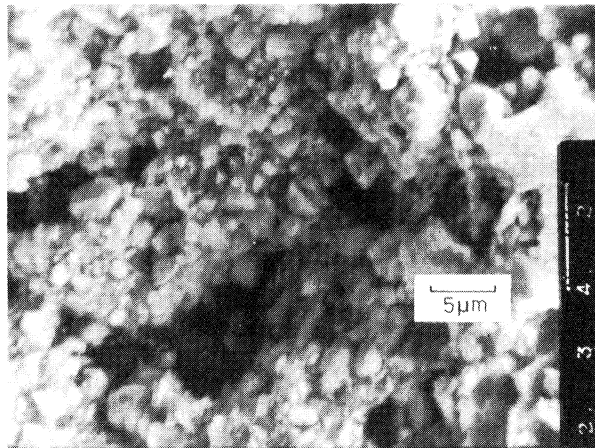


FIGURE 2 Du Pont 1111

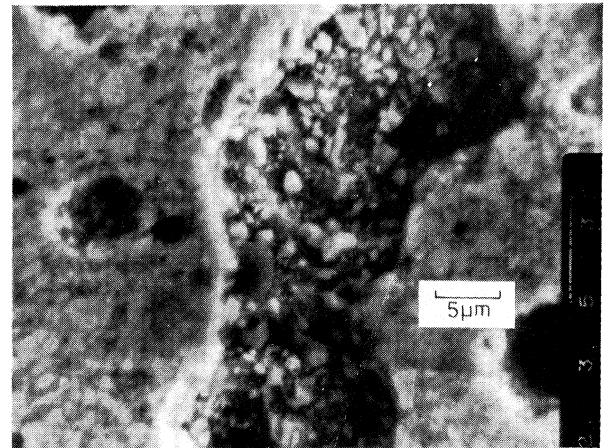


FIGURE 5 Du Pont 1121

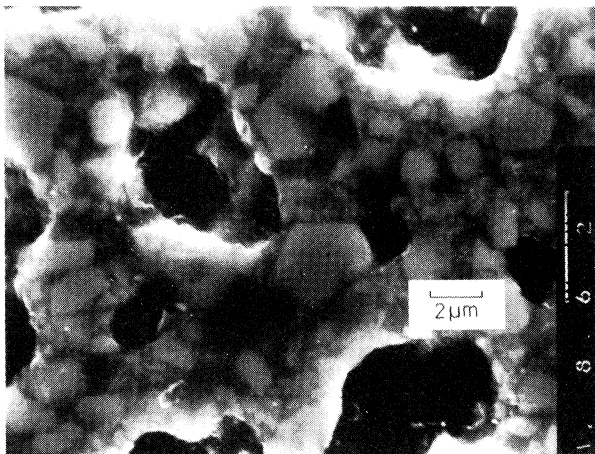


FIGURE 3 Du Pont 1111

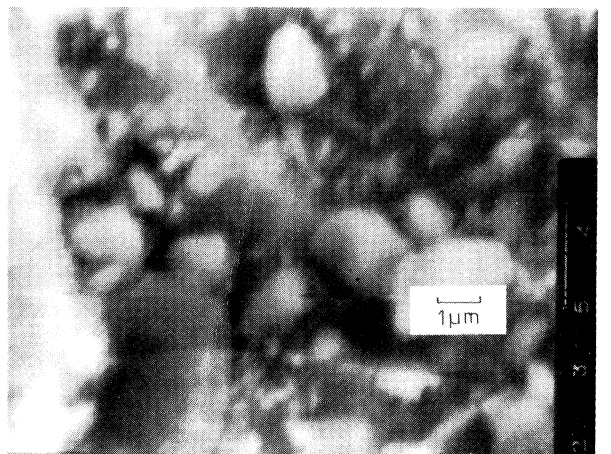


FIGURE 6 Du Pont 1121

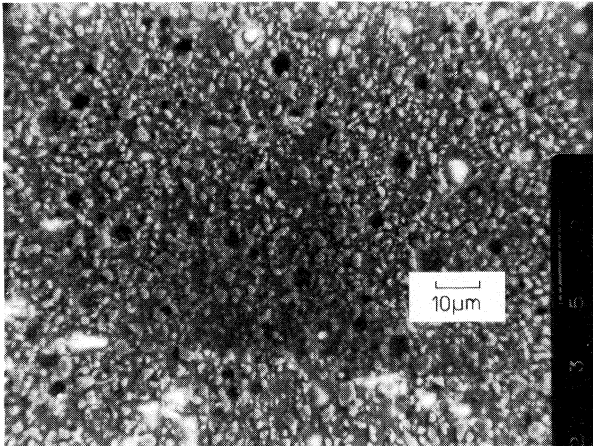


FIGURE 7 Du Pont 1131

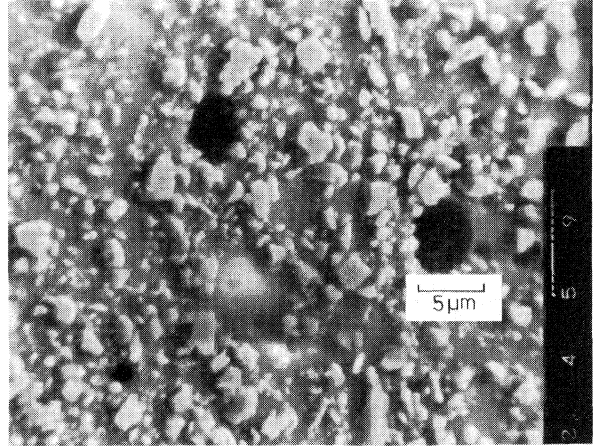


FIGURE 10 Du Pont 1141

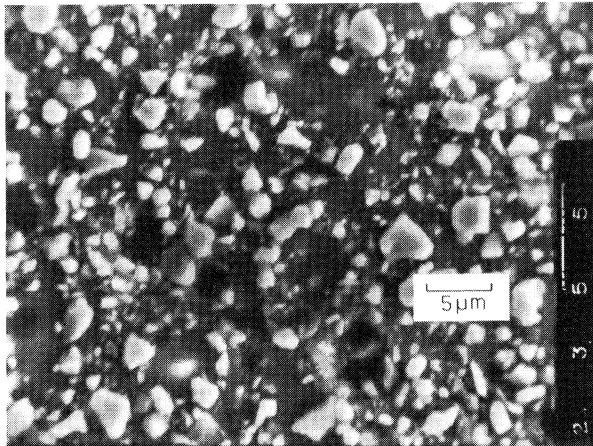


FIGURE 8 Du Pont 1131

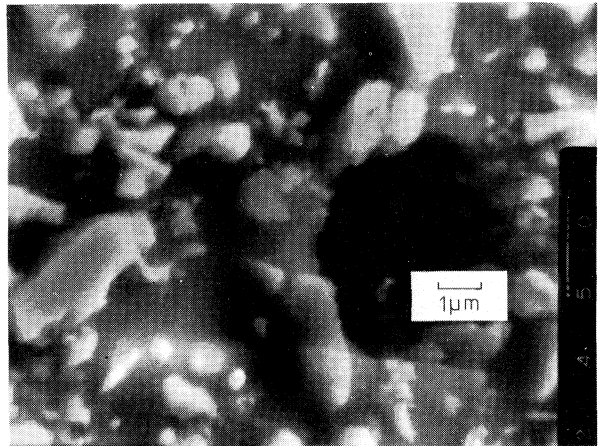


FIGURE 11 Du Pont 1141

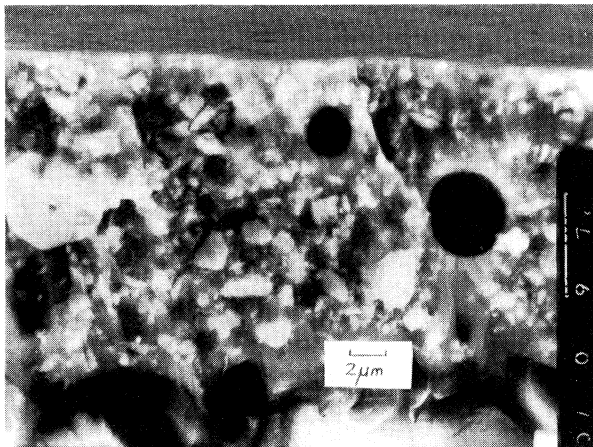


FIGURE 9 Du Pont 1131

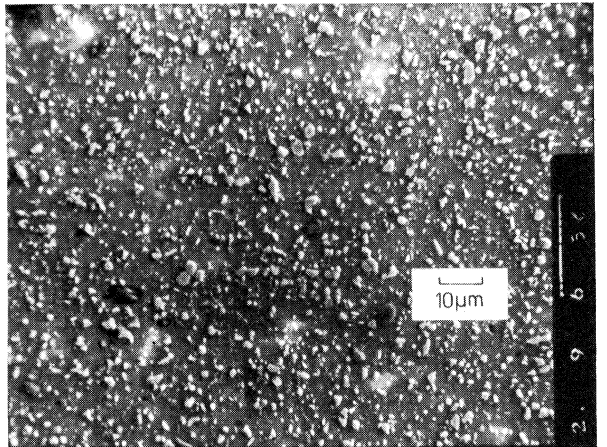


FIGURE 12 Du Pont 1151

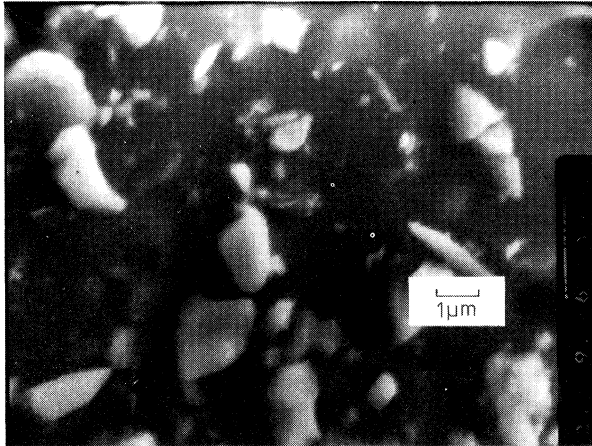


FIGURE 13 Du Pont 1151

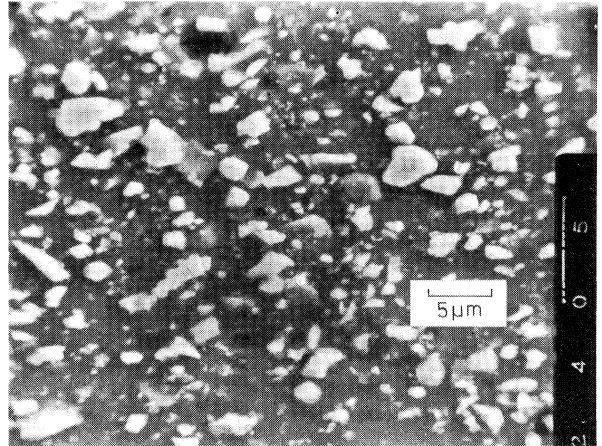


FIGURE 14 Du Pont 1161

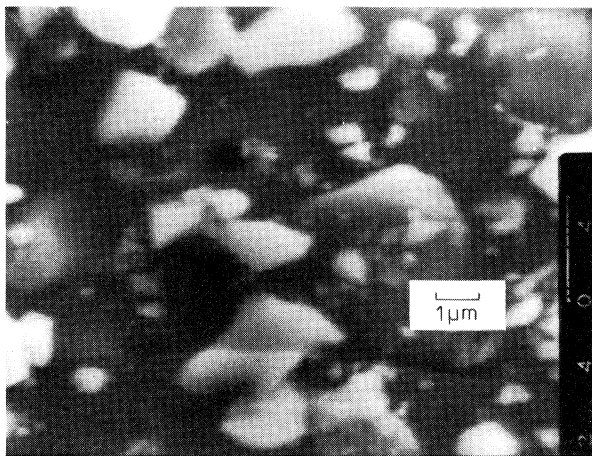


FIGURE 15 Du Pont 1161

which suggests the addition of CdO to the glass composition.

3.2 Alloys B Series

3.2.1. Micrographs It was necessary to tilt Alloys B samples through 45° in the SEM to improve resolution. EPMA took place with samples mounted normal to the electron beam.

R11B shows a very fine microstructure (Figure 17) which at higher magnification is seen to consist of approximately $0.25 \mu\text{m}$ particles, (Figure 18).

The $100 \Omega/\text{square}$ resistors (Figures 19 and 20) have a similar microstructure to R11B except that particles of up to $2 \mu\text{m}$ in width are dispersed amongst

the sub-micron particles seen in R11B. Figure 20 shows that the particles have an angular shape, which implies crystallinity.

R13B resistors revert to the small crystallite size microstructure of R11B (Figure 21). Voids are now spherical in shape rather than irregular (Figure 22) which shows that the higher resistivity ink is less viscous when fired due to a higher glass content. Broad chains of micro-particles surround particle-free areas of matrix material of up to $4 \mu\text{m}$ in width.

The R14B micrographs display areas of charging on the sample surface (Figure 23) for the higher resistivity material. Figures 23 and 24 show a filamentary network of micro-particles. The darker matrix material is charged, away from these particles, and is probably a poorly conducting glass. The shape of these filamentary paths of particles may have been defined by the size of the ball-milled glass particles in the resistor ink to which the smaller crystallites may have adhered. During the firing cycle the glass may melt and homogenise leaving particles frozen close to their original location when the glass resolidifies. Alternatively the particulate material may have come out of solution with the glass during the cooling stage of the firing cycle and the crystallites so formed are frozen into position as the glass cools. Figures 23 and 24 also have large particles of $1 \mu\text{m}$ to $4 \mu\text{m}$ in width distributed randomly over the resistor surface.

In $100 \text{ k}\Omega$ R15B resistors the micro-particles cease to form continuous chains across the sample surface (Figure 25). In three dimensions it is quite conceivable that continuous chains do occur.

No $1 \text{ M}\Omega/\text{square}$ Alloys B resistors were manufactured at the time of this work suggesting that for

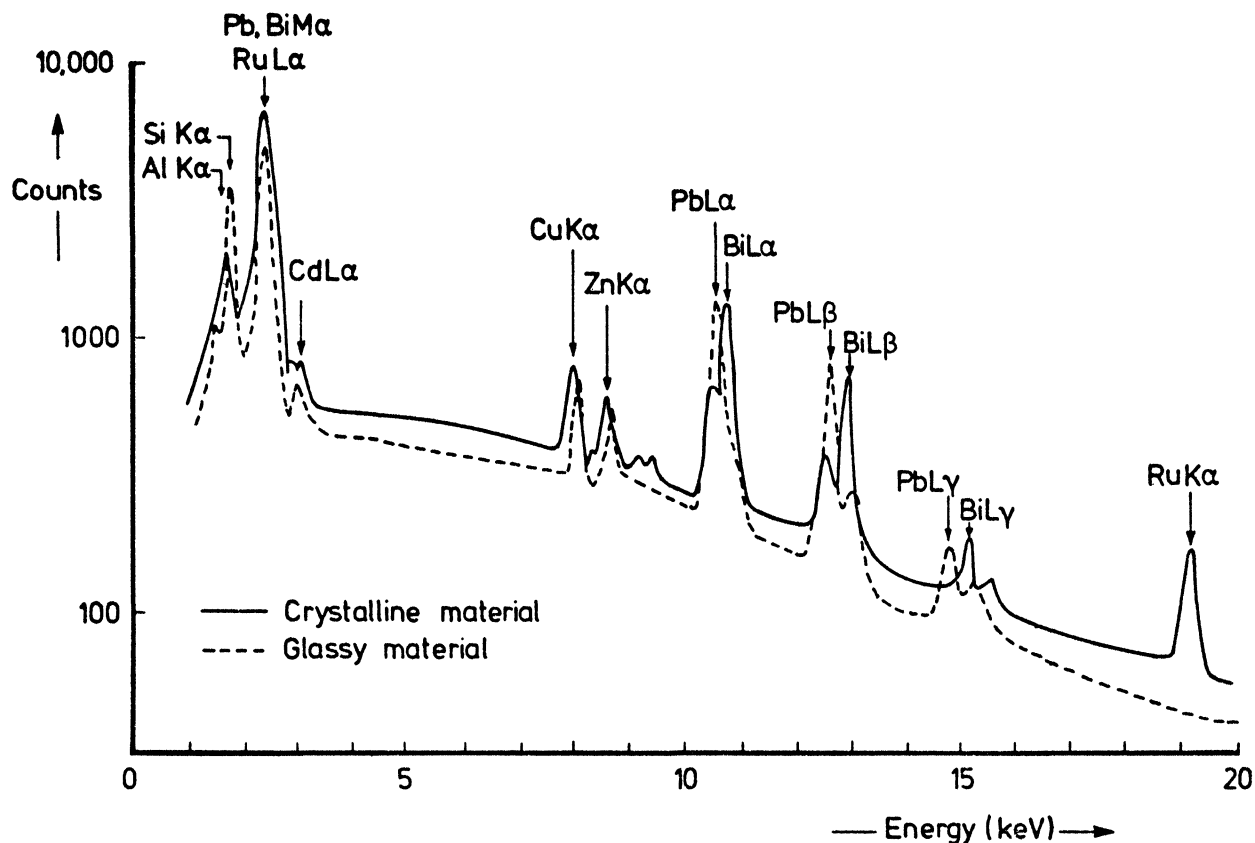


FIGURE 16 Du Pont 1161 Spectra

higher particle separations the resistivity approaches that of the glass.

3.2.2. Spectra The spectra for the Alloys B resistors are similar to those of the Du Pont 1100 series, with several important exceptions. There are no Bi peaks and Zr, Ag, In, Ba and Fe are also detected in small amounts.

Alloys B resistors were seen to consist of sub-micron size particles embedded in matrix material. A third phase of large crystallites was occasionally observed in R11B and R14B. All three phases were micro-probed. A large background from the small particulate phase was found in the spectra for the matrix phase and vice versa. However, the matrix spectra contain predominantly Pb and Si peaks and small Zr, Ag, In, Ba and Fe peaks. As with the 1100 resistors we assume the matrix to be a lead borosilicate glass with small additions, as dopants or impurities, of the elements or their oxides. The micro-

particles and large crystallites give similar spectra which contain strong Ru K and L peaks. The crystallites could therefore be metallic Ru, a Ru oxide or a mixed oxide such as PbO-RuO_2 . As many RuO_2 -based systems have been encountered in the literature^{3,4,5,6}, the particles are identified as the dioxide or a mixed oxide rather than Ru metal.

3.3 Electroscience 7000 Series

Two members of this series were surface-polished and investigated with the SEM and EPMA. Other members of the series from 7011 to 7016 were snapped and their sections electron-probed. The same elemental peaks were obtained for all the samples. These were Al(K), Si(K) and Pb(M and L) which were attributed to a glassy phase. A broad peak occurred from 2.84 keV to 2.98 keV coinciding with Pd and Ag L excitations. A small peak also appeared consistently for all specimens and it was identified as Ca K α .

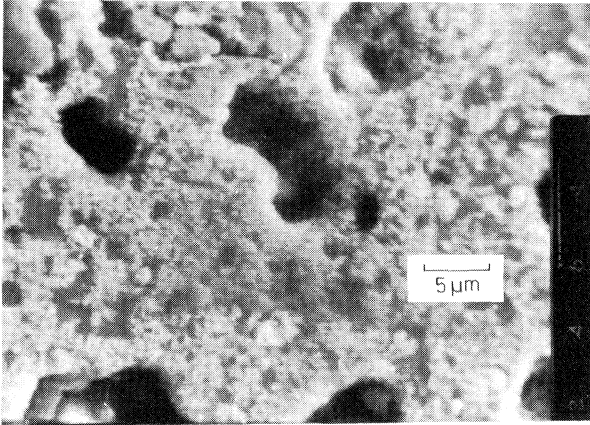


FIGURE 17 Alloys R11B

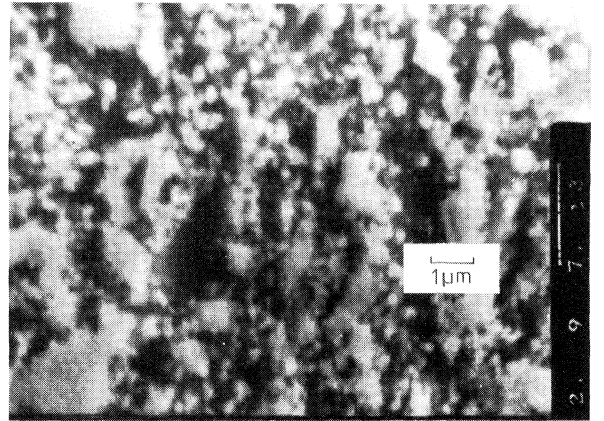


FIGURE 20 Alloys R12B

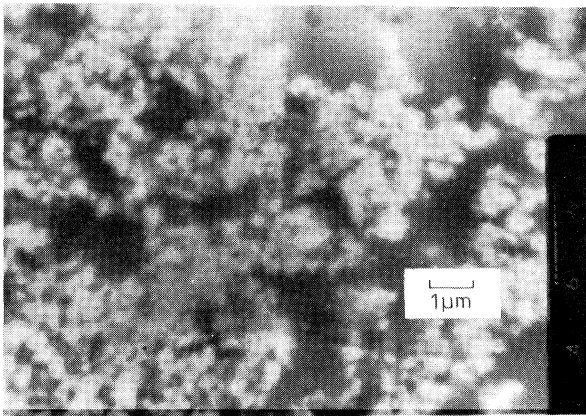


FIGURE 18 Alloys R11B

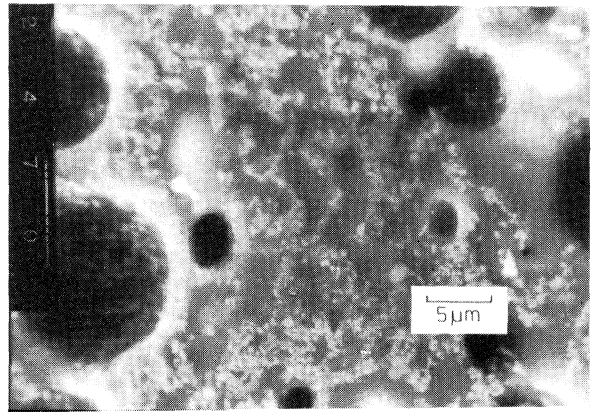


FIGURE 21 Alloys R13B

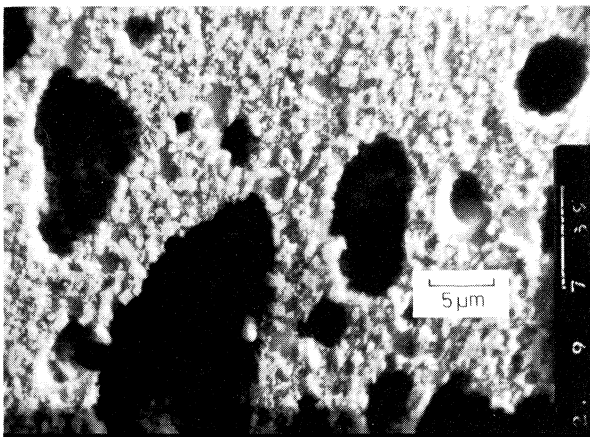


FIGURE 19 Alloys R12B

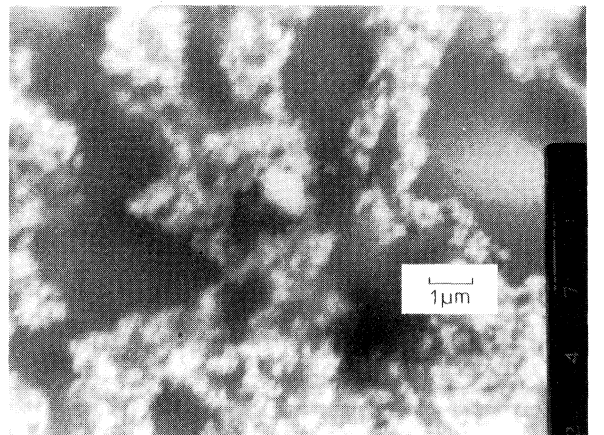


FIGURE 22 Alloys R13B

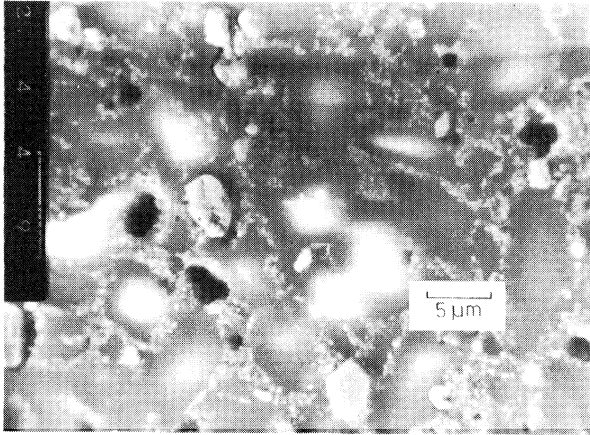


FIGURE 23 Alloys R14B

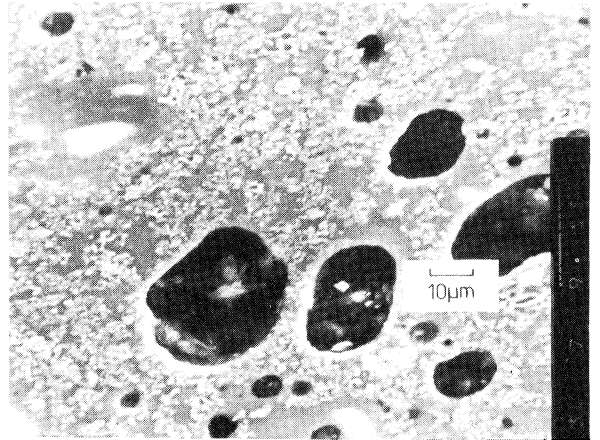


FIGURE 26 Electroscience 7013

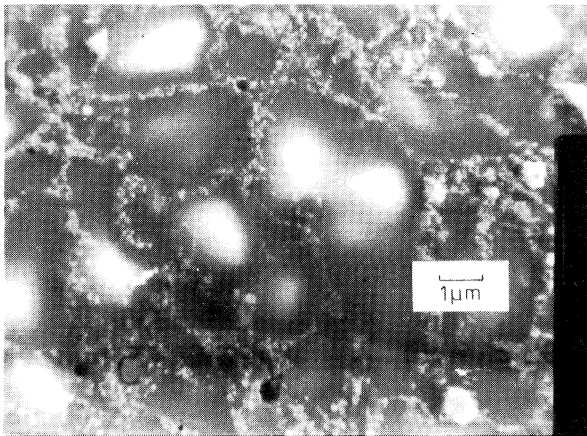


FIGURE 24 Alloys R14B

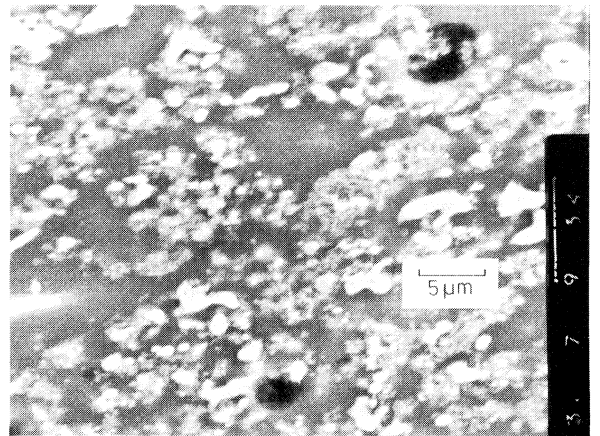


FIGURE 27 Electroscience 7013

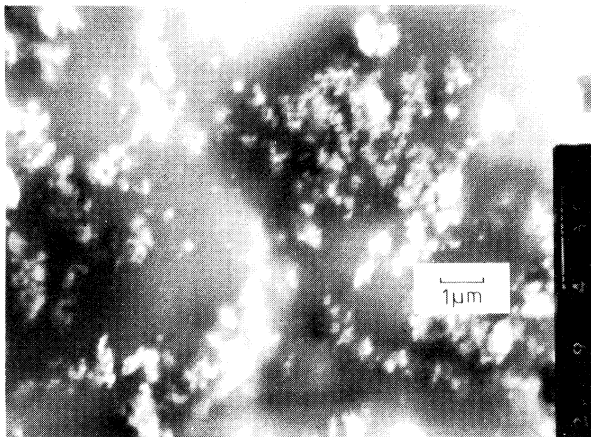


FIGURE 25 Alloys R15B

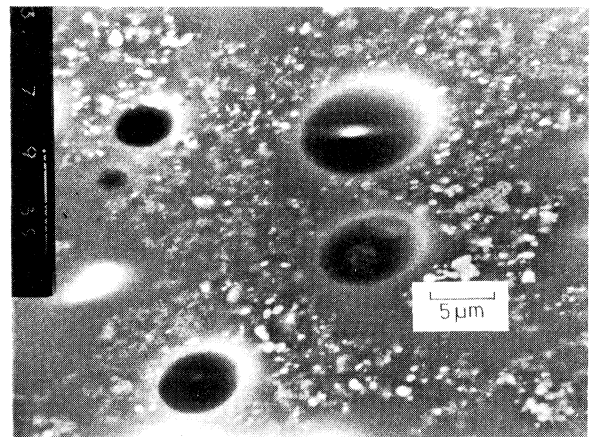


FIGURE 28 Electroscience 7014

Figure 26 shows the 7013 (1 k Ω /square) surface. A two-phase structure typical of the Alloys B series is seen. Micro-particles are dispersed in a dark matrix material and charging occurs on particle-free areas of the sample surface. Voids from 2 μ m to 30 μ m in diameter are in random positions on the surface. Figure 27 reveals the particle sizes and spacings. Two particle sizes are discernible; sub-micron and larger fragments from 0.5 μ m to 2 μ m in diameter. Individual probing of the large particles gave a strong Pd/Ag peak.

The 10 k Ω /square resistor 7014 has a similar microstructure (Figure 28) to 7013. The density of particles is now lower, and larger areas of the sample surface are particle-free. Elliptical voids seen are in fact circular, as the sample is tilted at 45°.

The 7000 series is a relatively early one and is identified as a Pd/Ag system. Ca may be added as CaO to the glassy phase which is a lead or lead-alumino borosilicate glass. Particles are in continuous contact and the sample resistivity is controlled by the number of paths available for conduction.

Part II of this paper continues with a materials survey of the TFR phases identified in Part I. Con-

duction in multiphase materials is then considered, and low TCR conduction processes are discussed. Finally conduction processes for the observed structures are proposed, and they are shown to be appropriate for TFRs with resistivities covering at least six orders of magnitude.

ACKNOWLEDGEMENTS

This work was carried out with the support of Procurement Executive, Ministry of Defence at the Dept. of Physics, Chelsea College, London. Permission from the MoD to publish this work is gratefully acknowledged.

REFERENCES

1. D. A. Cash, M. P. Ansell and R. M. Hill, 1974. Final Report MoD Contract No. RU7-41.
2. M. V. Coleman and P. W. Graves, 1972. Third Report RCRDC Contract No. K27A/486/CB27A/2.
3. H. C. Angus and P. E. Gainsbury, *Electronic Components*, **9**, 84 (1968).
4. G. S. Iles, *Radio and Electronic Engineer*, **11**, 299 (1968).
5. P. R. van Loan, *Insulation/Circuits*, **6**, 35 (1972).
6. T. H. Lemon, *Chemistry and Industry*, **19**, 920 (1973).



Hindawi

Submit your manuscripts at
<http://www.hindawi.com>

